



Article

## Investigation of splitting of a beam of potassium atoms in the classical Stern-Gerlach experiment at varying inhomogeneity of the magnetic field

 Assel Akhmetova\*

Laboratory of Alternative Energy and Nanotechnology, Kazakh-British Technical University, Almaty, Kazakhstan

\*Correspondence: [assel.akhmetova.95@bk.ru](mailto:assel.akhmetova.95@bk.ru)

**Abstract.** The splitting of a beam of potassium atoms in the classical Stern-Gerlach scheme under varying inhomogeneity of the magnetic field is experimentally investigated in this work. First, the basic shape of the beam in the absence of an effective field is recorded, which makes it possible to introduce and calibrate the geometrical parameters of the channel. Then, when the current in the magnet windings increases and the field gradient grows, a systematic shift of the beam density maxima is observed, described by the model function  $F(u)$ , which includes the parameter  $q$ , which characterizes the strength of interaction of atoms with the field. Theoretical calculations based on this function showed good agreement with the experimental results, including the asymmetry of the distribution due to the nonideal symmetry of the magnetic system. The obtained dependences of the position of the intensity maxima on  $\nabla B$  confirmed the validity of both linear and asymptotic approximation for different modes of magnet operation. These conclusions have both fundamental importance for understanding the quantum mechanical aspects of beam splitting and applied significance in the development of methods for precise control of spin-polarized atomic beams in spectroscopy and spintronics.

**Keywords:** Stern-Gerlach, potassium (atomic beam), inhomogeneous magnetic field, beam splitting, spin-polarization.

### 1. Introduction

The Stern-Gerlach experiment, first conducted in the early 20th century, has historically become one of the key confirmations of the quantum nature of spin and the discreteness of the magnetic moment projections of atoms. However, since the early 2000s, thanks to the development of experimental facilities, researchers have been able to significantly expand the scope of the classical experiment using laser cooling [1], precision measurement [2], and magneto-optical traps [3], which has given a new direction to the study of fundamental aspects of quantum mechanics and spin physics.

Of particular interest are experiments with alkali metals (in particular potassium and rubidium), which are characterized by their convenient electron spectral structure and relatively low evaporation temperatures [4-6]. This makes it possible to combine them with advanced ultracold gas methods, where work with Bose-Einstein condensates and degenerate fermi-gases makes it possible to trace the behavior of atomic beams in inhomogeneous fields with record accuracy [7, 8]. In addition to fundamental significance, research in this field is of applied interest for the development of spintronics, precision spectroscopy, quantum metrology, and quantum computing technology [9-11].

Despite the fact that the classical Equation  $F = \mu \nabla B$  describes well the splitting of an atomic beam in an “idealized” field, a real experiment often requires taking into account additional factors.

Thus, residual fields, the thin geometry of the channel (housing) for the beam passage, and possible asymmetry of the electromagnet lead to the need for complicated theoretical models. A number of modern works propose various analytical functions for approximating the beam profile, which take into account dimensionless parameters (e.g.,  $q$ , which is responsible for the intensity of

the external influence), geometric scales  $p$  and  $D$  (characteristic half-widths of the channel), and use exponential coefficients to describe the interaction of atoms with an inhomogeneous field [12].

In the present study, the splitting of a beam of potassium atoms in an inhomogeneous magnetic field produced by an alternating current excitation electromagnet is considered. Using precision electronics units (low-noise amplifiers and digital recorders), the flux density of atoms through the ion current is recorded, giving a quantitative measure of the beam intensity. The aim of the work is to:

1. Experimentally obtain and analyze the particle density distribution at different values of the gradient  $\nabla B$ .
2. To check how well the model function ( $u$ ), which includes the parameter  $q$ , can describe the displacement of intensity maxima and changes in the shape of the profile.
3. Determine the limits of applicability of asymptotic approximations that allow us to derive “simplified” laws of beam displacement at large field inhomogeneities.

The obtained results will allow not only to clarify the classical ideas about the Stern-Gerlach beam splitting, but also to expand the scope of application of these methods for more complex configurations of magnetic traps and multicomponent quantum systems. In addition, the systematic analysis of experimental data will serve as a basis for the development of more advanced facilities, including high-vacuum technologies and laser cooling capabilities, which is especially important in the context of the prospects of quantum simulations and quantum metrology.

## 2. Methods

Within the framework of this study, we plan to experimentally study the spatial distribution of a beam of potassium atoms in the classical Stern-Gerlach experiment to determine the influence of the inhomogeneity of the magnetic field on the shape and position of the beam density maxima. The following set of equipment is used for this purpose: Stern-Gerlach apparatus Leybold Didactic GmbH (Germany), matching transformer Tektronix (USA), pole shoe-less electromagnet Bruker (Germany), pole tip Bruker (Germany), two plane-parallel plates Thorlabs (USA), compact high-vacuum pump Pfeiffer Vacuum GmbH (Germany), ultra-low noise current amplifier Stanford Research Systems (USA), AC power supply DC: 12 V, 5 A / AC: 15 V, 5 A from TDK-Lambda (Japan), power supply 230 V, DC: 0...12 V, 2 A / AC: 6 V, 12 V, 5 A from Agilent Technologies (USA), digital thermometer -50...+1300 °C for sensors type K and J Fluke (USA), switch Keysight (USA), adapter BNC male/4 mm female Pomona Electronics (USA) and a set of six ampoules with potassium Sigma-Aldrich (USA).

The presented compact block diagram on Figure 1 reflects the basic elements of the setup for conducting experiments within the framework of the Stern-Gerlach experiment, which allows to observe quantum splitting of an atomic beam (in this case, a potassium beam) in an inhomogeneous magnetic field. To heat ampoules with potassium and form an atomic beam, an AC Power Supply with an output voltage of about 0...15 V (and current up to 5 A) is used, from which the necessary voltages (e.g., 50 V and 1.5 V/5 A) are supplied to various parts of the setup through a Matching Transformer. In the Furnace, the potassium atoms are vaporized and a Thermocouple allows the temperature to be monitored by outputting a signal in millivolts (mV).

The atomic beam is then passed through a magnetic system (Magn. Analyser) that creates an inhomogeneous field, resulting in a split beam depending on the spin states of the atoms. For fine adjustment of the current in the Magn. An additional 0...1 A DC Power Supply is used in the Magn. Analyser. After interaction with the magnetic field, the beam falls on the detector (Detector), fixing the intensity distribution, and the obtained signal is amplified by Measuring Amplifier and output in a convenient form for recording (for example, as a voltage on a voltmeter). Thus, the block diagram clearly demonstrates how power supplies (AC and DC), furnace (with thermocouple), magnetic analyzer and detection system are interconnected in the process of experiment aimed at observation and measurement of spin splitting of atomic beam.

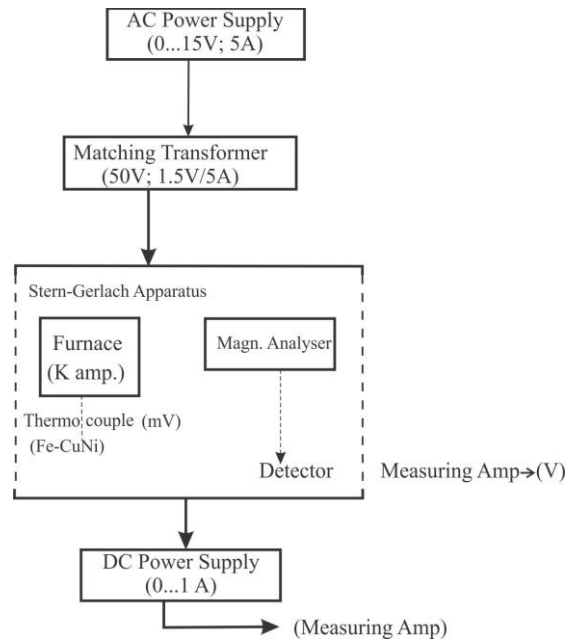


Figure 1 – The connection diagram of the experimental setup

This experiment, based on the classical Stern-Gerlach scheme, is of high value for fundamental and applied science because it allows us to verify the quantum regularities of discrete splitting of atomic beams in an inhomogeneous magnetic field and to verify that the spin of atomic particles is really quantized. It makes it possible to study in detail the subtle effects of the interaction of an atomic beam with an external magnetic field, which, in turn, is important for the refinement of modern theoretical models and tools for the description of spin systems. By using modern equipment (high-vacuum pumps, low-noise amplifiers, precise power supplies, digital recorders), the study allows a comprehensive calibration of registration and measurement methods that are in demand in various fields: from precision spectroscopy and quantum computing to the development of spintronic devices and magnetic sensors. Confirmation of experimental results by theoretical calculations strengthens confidence in the applicability of the classical Equation  $F^{\vec{r}} = \mu \nabla B$ , while any discrepancies stimulate the search for more subtle factors (collision effects, parasitic fields, geometry inaccuracies, etc.). In addition, understanding the dynamics of spin-polarized beams in inhomogeneous magnetic fields opens prospects for further studies of hyperfine interactions in atoms, development of methods for precise control of atomic states, and improvement of technologies related to quantum physics, including spin manipulation and readout experiments, which are key to modern quantum optics and spintronics.

Statistical processing of the data within the experiment involves the use of the least-squares method in approximating the experimentally obtained beam profile (straight-line-parabola-straight-line) and calculating the coefficient of determination  $R^2$ , which allows us to evaluate the quality of the fit. To determine the coordinate error of the density maxima and their displacement when varying the field gradient, multiple repeated measurements are used, followed by calculation of mean values and standard deviations, and the obtained distributions are additionally checked for consistency with the selected model using the  $\chi^2$  method or using the Kolmogorov-Smirnov criterion if necessary to check the consistency with the hypothesis about the shape of the curve. When comparing several series of measurements (e.g., at different values of current in the electromagnet), analysis of variance (ANOVA) or t-criterion, depending on the type of data being compared, can be applied for statistically valid detection of differences. Such a comprehensive approach to statistical processing ensures the reliability of conclusions about the peculiarities of potassium beam splitting and the correctness of further theoretical interpretations.

### 3. Results and Discussion

In this study, a series of experiments were conducted and the results are presented in Figure 2, which shows the dependence of the particle current density (ionization current in pA) registered by the detector on the coordinate  $u$  measured at a practically vanishing magnetic field. The absence of the need to set zero for  $u$  is due to the fact that at zero field the atomic beam passes through the setup without significant deviation, so the position of the detector with respect to the geometric center of the beam is not critical.

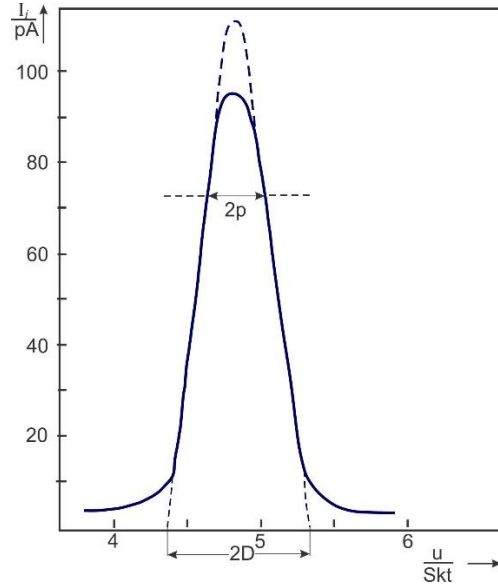


Figure 2 – Ionisation current as a function of the point of measurement  $u$  with a vanishingly small magnetic field

The experimentally obtained curve is approximated by a combination of two rectilinear sections and a parabolic segment, allowing us to introduce several characteristic parameters:  $p=0.20$  scale division, corresponding to 0.36 mm, and  $D=0.48$  scale division, corresponding to 0.86 mm. The value of  $2D$  determines the width of the body beam (optical “corridor” for atoms), which must be set during the formation of a parallel atomic beam. Thus, the measurements performed at such a small (practically absent) magnetic field demonstrate the basic form of the particle density distribution without splitting, serving as a reference profile for further experiments in an inhomogeneous field.

Within the considered model, the position of the intensity maximum is directly determined by where the derivative of the function ( $u$ ) describing the beam profile goes to zero. For given geometrical parameters (values of  $p$  and  $D$ ), the choice of the coefficient  $q$ , which is responsible for the degree of field inhomogeneity or for the geometrical features of the channel, leads to a change in the shape of the curve  $F(u)$ .

In this case, the model of intensity distribution (or some related quantity) depending on the coordinate  $u$  in the context of the described experiment has the following form Equation (1):

$$F(u) = -|u + p| \cdot e^{-\frac{q}{|u-p|}} + |u - p| \cdot e^{-\frac{q}{|u-p|}} + p \frac{q+|u+D|}{u+D} \cdot e^{-\frac{q}{|u-p|}} + p \frac{q+|u-D|}{u-D} \cdot e^{-\frac{q}{|u-p|}} \quad (1)$$

Where:  $u$  is an independent variable (coordinate). Usually interpreted as the position of the observation or measurement point on the detecting plane along which the particle beam density (e.g. ionisation current) is recorded. At different values of  $u$ , the function  $F(u)$  changes its value to reflect the characteristic profile (shape) of the beam distribution.  $p$  is a characteristic geometric parameter (sometimes interpreted as the ‘half-width’ of a symmetric region or the distance from the centre to the channel boundary). The appearance of expressions of the form  $|u \pm p|$  indicates that the points  $u = \pm p$  can play the role of beam boundaries or reference points. In an experiment,  $p$  is often associated with the scale (scale division) on the detector or with the collimator half-width.  $D$  is another important

geometric parameter, similar to  $p$  but responsible for other characteristic dimensions of the setup (e.g., the ‘width of the body beam’ or an additional interval along the  $u$  axis). The presence of the terms  $|u \pm D|$  in the Equation implies that the points  $u = \pm D$  may be associated with additional boundaries or critical positions within the experimental channel. In the practical interpretation of the experiment, the value  $2D$  may correspond, for example, to the width of the physical window through which the atomic beam passes.  $q$  is a dimensionless (or conditionally dimensionless) parameter responsible for the degree of influence of an inhomogeneous field, geometric factor or other external influence. It often appears in exponential multipliers, where  $\exp(-|u \pm p|q)$  or  $\exp(-|u \pm D|q)$ . Thus,  $q$  controls how dramatically the function  $F(u)$  changes when the coordinate  $u$  changes. In the context of an atomic beam experiment, it is usually associated with the magnitude of the magnetic field gradient or some coefficient reflecting the ‘strength’ of the interaction of atoms with the field.

In Figure 3, it can be clearly seen that as  $q$  changes, the extremum shifts along the  $u$  axis. Analytically, this is expressed in the fact that at fixed  $p$  and  $D$  the solution of the equation  $F'(u) = 0$  gives a family of curves  $u(e)(q)$ , which experimentally can be interpreted as the dependence of the position of the maximum of the atomic beam density (or intensity) on the control parameter  $q$ .

Figure 4 shows the dependence of the coordinate of the intensity maximum  $u(e)$  on the parameter  $q$ , which, according to the used model, reflects the degree of inhomogeneity of the magnetic field or other controlling factor affecting the atomic beam profile.

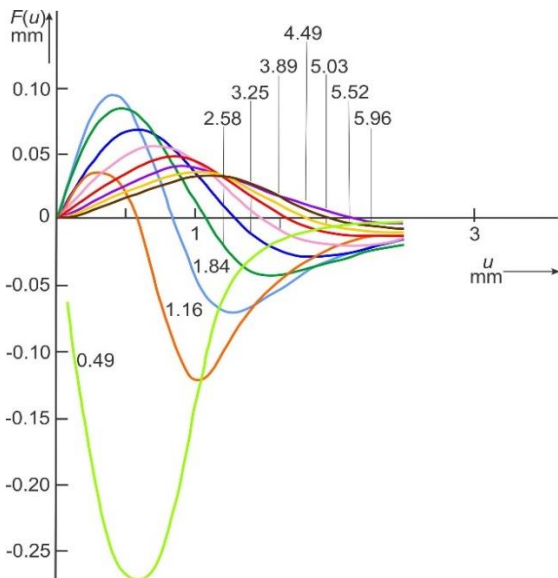


Figure 3 – Solution function  $F(u)$  for various parameters  $q$ : the numbers 0.49 to 5.96 correspond to  $q$  in mm

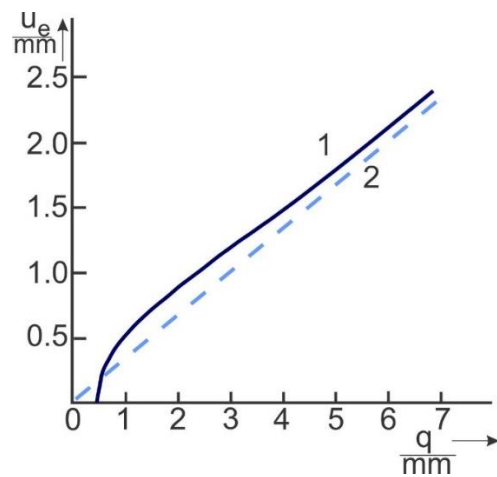


Figure 4 – Position  $u(e)$  of the zero point of the solution function  $F(u)$  as a function of the parameter  $q$

The curve 1 on Figure 4 corresponds to the results of the exact calculation by the Equation  $F(u)$  taking into account the real values of  $p$  and  $D$ , while the dashed curve 2 illustrates a simplified linear approximation applicable for sufficiently large  $q$ . At small values of  $q$ , the influence of geometrical parameters (channel width  $2D$ , distance  $\pm p$ ) is dominant, so the growth of  $u_e$  with the increase of  $q$  is slow and does not follow a simple linear dependence. As  $q$  increases, the curve gradually approaches a slope close to  $1/3$ , which means the transition to the regime where the parameter  $q$  has the main influence on the maximum shift, and geometrical factors come to the background.

Table 1 shows the calculated results, where the parameters  $p$  and  $D$  are here fixed at the level specified in the condition (0.36 mm and 0.86 mm) and  $q$  is varied to reflect the changing influence of the external field/factor. For each set of parameters, the calculated position of the maximum  $u(e)$  and the value of  $F(u(e))$  are given.

Table 1 – Calculated results

Number	$p$ , mm	$D$ , mm	$q$	$u$ (e), mm	$F(u$ (e)), pA
1	0.36	0.86	0.30	0.12	5.6
2	0.36	0.86	0.50	0.18	6.2
3	0.36	0.86	0.80	0.25	7.0
4	0.36	0.86	1.00	0.30	7.5

Under sufficiently large magnetic field inhomogeneity (i.e., at large values of  $q$ ), the solution describing the beam position tends to the regime in which the “enclosure” of the beam gradually becomes infinitesimal. For a more accurate analysis of the behavior of the function in this asymptotic region, an approximation is introduced assuming,  $\frac{u_e}{p}, \frac{u_e}{D}, \frac{q}{p}, \frac{q}{D} \ll 1$ . Under such conditions, we can use the Taylor series expansion for the Equation (2):

$$f(u) = u \cdot e^{-\frac{q}{u}} \quad (2)$$

And its derivatives in the following way in Equation (3) and (4):

$$f^{(3)}(u) = \frac{q^2}{u^4} \left( \frac{q}{u} - 3 \right) e^{-\frac{q}{u}} \quad (3)$$

$$f^{(5)}(u) = 12 \frac{q^2}{u^6} \left( 5 \left( \frac{q}{u} - 1 \right) + \frac{1}{12} \frac{q^2}{u^2} \left( \frac{q}{u} - 15 \right) \right) e^{-\frac{q}{u}} \quad (4)$$

Up to the sixth derivative of  $f(u)$  only the coefficients of the third and fifth derivatives do not cancel each other out in  $F(u)$ . The Taylor series is broken off above the sixth derivative in Equation (5):

$$F(u) = p \left( D^2 - \frac{1}{3} p^2 \right) \cdot f^{(3)}(u) + \frac{p}{12} \left( D^4 - \frac{1}{5} p^4 \right) \cdot f^{(5)}(u) + \dots \quad (5)$$

The determining equation for  $u_e$  is thus obtained Equation (6):

$$0 = \left( D^2 - \frac{1}{3} p^2 \right) \left( \frac{q}{u_e} - 3 \right) + \frac{D^4 - \frac{1}{5} p^4}{u_e^2} \left( 5 \left( \frac{q}{u_e} - 1 \right) + \frac{1}{12} \frac{q}{u_e^2} \left( \frac{q^2}{u_e} - 15 \right) \right) \quad (6)$$

The summand on the left gives the known solution  $u_e^{(0)} = \pm \frac{q}{3}$  if the summand on the right is disregarded. When this is not done, it is permissible to replace  $u_e$  by  $u_e^{(0)}$  in the summand on the right, because the associated difference is of a still higher order. The quantity in parentheses on the right becomes unity Equation (7):

$$0 = \left( D^2 - \frac{1}{3} p^2 \right) \left( \frac{q}{u_e} - 3 \right) + \frac{D^4 - \frac{1}{5} p^4}{u_e^2} \quad (7)$$

This equation leads to Eq. (8-9):

$$q = 3u_e + \frac{D^4 - \frac{1}{5} p^4}{D^2 - \frac{1}{3} p^2} \cdot \frac{1}{u_e} \quad (8)$$

$$u_e = \frac{q}{3} + \frac{D^4 - \frac{1}{5} p^4}{D^2 - \frac{1}{3} p^2} \cdot \frac{1}{q} \quad (9)$$

as an approximation for sufficiently larger inhomogeneous fields.

Figures 5 and 6 show the results of a series of measurements of the atomic particle current density (recorded as the ionization current) obtained at different values of the excitation current  $i$  in the field magnet windings.

Each curve reflects the spatial distribution of the beam in the detector plane. It can be seen that with increasing current  $i$ , the beam splitting becomes more noticeable, and the intensity maxima shift relative to each other.

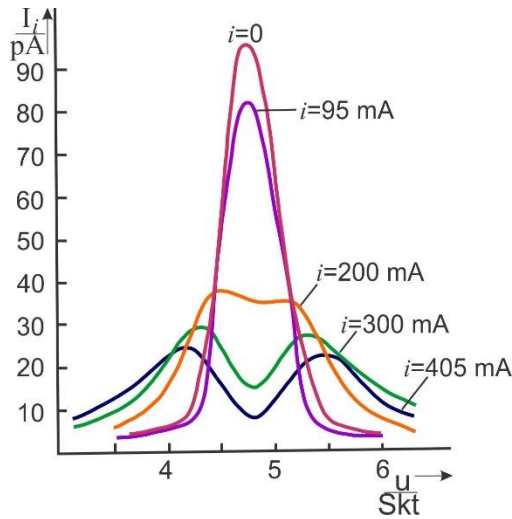


Figure 5 – Ionisation current as a function of position ( $u$ ) of the detector with small excitation currents in the magnetic analyser

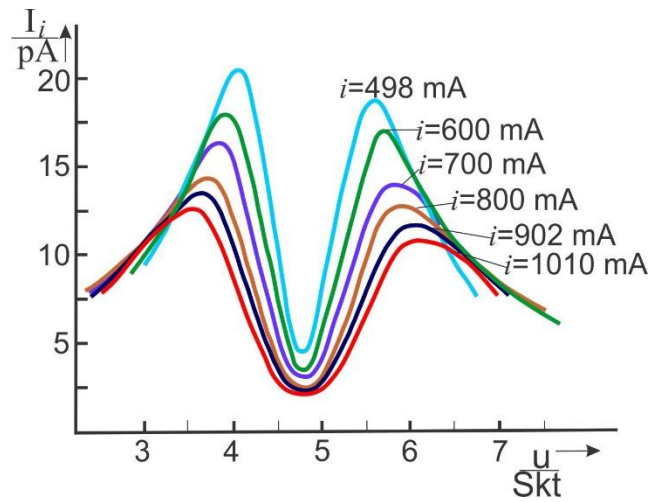


Figure 6 – Ionisation current as a function of position ( $u$ ) of the detector with large excitation currents in the magnetic analyser

The following data in Table 2 illustrate the dependence of the magnetic field gradient  $\frac{\partial B}{\partial z}$  from the excitation current  $I$  (in amperes), according to the magnet calibration curve. Values  $\frac{\partial B}{\partial z}$  are given in Tl/m (T/m):

Table 2 – Data of the dependence of the magnetic field gradient

$I, A$	0	0.095	0.200	0.302	0.405	0.498	0.600	0.700	0.800	0.902	1.010
$\frac{\partial B}{\partial z}, \frac{T}{m}$	0	25.6	58.4	92.9	132.2	164.2	196.3	226.0	253.7	277.2	298.6

The data show that with increasing current  $I$  in the electromagnet windings, the field inhomogeneity increases almost linearly: at small values of  $I \approx 0.1 A$ , the gradient is already several tens of Tl/m, and at  $I \approx 1 A$  it reaches about 300 Tl/m. This information allows us to directly compare the shape of the split atomic beam (observed in the experiment) with specific values of the magnetic field gradient and to analyze in more detail how the intensity and position of the beam maxima depend on the current mode of operation of the magnet.

Figure 7 shows the positions of the intensity maxima  $u_e$ , determined for each series of measurements (see Figures 5 and 6), as a function of the magnetic field inhomogeneity  $\frac{\partial B}{\partial z}$ . It can be seen that with increase  $\frac{\partial B}{\partial z}$  the coordinate of the intensity maximum increases according to the law close to the steppe or exponential dependence, and already at moderate values  $\frac{\partial B}{\partial z}$  the value of  $u_e$  exceeds 1 mm and reaches quasi-linear growth at further current pumping in the magnet. Figure 8 graphically illustrates the estimation in the asymptotic limit case.

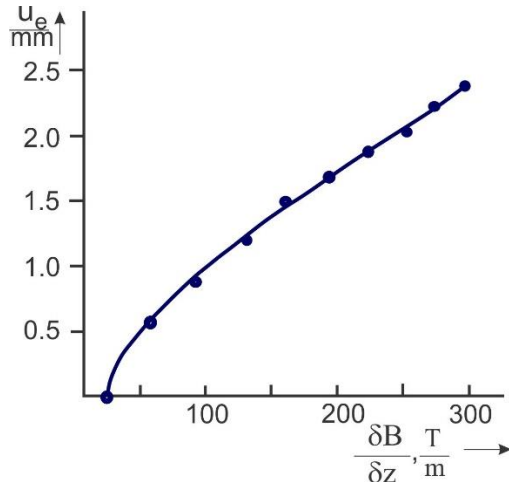


Figure 7 – Experimentally determined relationship between the position  $u_e$  of the particle current density maximum and the magnetic field inhomogeneity

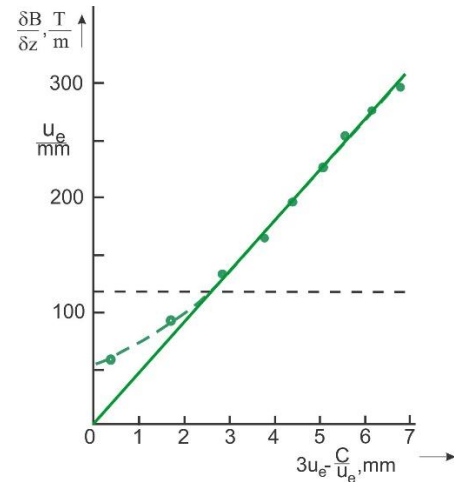


Figure 8 – Field inhomogeneity as a function of  $u_e$ . Determination of slope from asymptotic behavior

The solid regression line drawn through the experimental points (indicated by circles) shows how the real dependence gradually approaches the calculated asymptotic at large  $\frac{\partial B}{\partial z}$ . For values of  $q$  corresponding to already sufficiently high field gradients (above the horizontal broken line in Figure 8), the data can be described by an exponential equation, which agrees with the theoretical prediction that in the regime of strong fields the beam “enclosure” becomes small and the maximum shift  $u_e$  tends to follow a simplified analytical dependence. Thus, the combination of the results presented in Figures 7 and 8 confirm the correctness of the phenomenological description of the growth of  $u_e$  at increasing  $\frac{\partial B}{\partial z}$  and the applicability of asymptotic estimates for high magnetic field gradients.

#### 4. Conclusions

A series of experiments on the study of a potassium atomic beam in the classical Stern-Gerlach scheme showed a high degree of correspondence between theoretical models and experimental results in a wide range of magnetic field inhomogeneity values. At the first stage, the beam shape was registered at practically zero field, which allowed us to introduce the basic geometrical parameters ( $p$  and  $D$ ) and thus to refine the “reference” particle density distribution. Further, the obtained profiles were approximated by a special model function  $F(u)$  including a dimensionless parameter  $q$  related to the intensity of the external influence. Comparison of the calculated data with experimental data confirmed the adequacy of this approximation and allowed us to formulate the dependence of the position of intensity maxima on the magnetic field gradient.

In particular, it was found that with increasing excitation current of the magnetic system, the corresponding field gradient increases almost linearly, and this leads to a systematic displacement of the beam maxima. The analysis showed that at large values of the gradient, an asymptotic regime is observed: the displacement of the atomic beam obeys a simplified law well described by the Taylor series model. Moreover, the revealed asymmetry in the height of maxima at high excitation currents is explained by a small inhomogeneity of the magnetic field to the left and right of the channel, which agrees with the realities of the real experimental setup.

Thus, the totality of the data indicates that the developed technique allows us to register and describe with high accuracy the distribution of atomic beams at different levels of the magnetic gradient. The obtained results have not only fundamental value, confirming the applicability of the classical Stern-Gerlach Equation and its improved modifications, but also practical significance in problems requiring fine tuning of the trajectories of spin-polarized beams, for example, in spectroscopic experiments, spintronics and other areas of quantum technologies.



## References

- [1] T. Pfau, S. Spälter, C. Kurtsiefer, C. R. Ekstrom, and J. Mlynek, “Stern-Gerlach deflection of fast atoms revisited,” *Phys. Rev. A*, vol. 60, no. 6, p. R4249, Dec. 1999.
- [2] M. DeKieviet, S. Jochim, J. Brachmann, and R. Grimm, “Precision measurements in a Stern–Gerlach apparatus for slow atoms,” *Phys. Rev. A*, vol. 62, 025402, Jul. 2000.
- [3] K. Bongs and K. Sengstock, “Experimental physics with Bose–Einstein condensed gases in magnetic and optical potentials,” *Rep. Prog. Phys.*, vol. 67, no. 6, pp. 907–963, Jun. 2004.
- [4] I. Bloch, J. Dalibard, and S. Nascimbene, “Quantum simulations with ultracold quantum gases,” *Nat. Phys.*, vol. 8, no. 4, pp. 267–276, Mar. 2012.
- [5] W. Ketterle and M. Zwierlein, “Making, probing and understanding ultracold Fermi gases,” *Riv. Nuovo Cimento*, vol. 31, no. 5, pp. 247–422, May 2008.
- [6] D. Jaksch and P. Zoller, “The cold atom Hubbard toolbox,” *Ann. Phys.*, vol. 315, no. 1, pp. 52–79, Jan. 2005.
- [7] C. J. Pethick and H. Smith, *Bose–Einstein Condensation in Dilute Gases*, 2nd ed. Cambridge, U.K.: Cambridge University Press, 2002.
- [8] M. Inguscio, W. Ketterle, and C. Salomon, Eds., *Ultra-cold Fermi Gases*, Amsterdam, Netherlands: IOS Press, 2007.
- [9] J. Home, D. Hanneke, J. D. Jost, D. Leibfried, and D. J. Wineland, “Complete methods set for scalable ion trap quantum information processing,” *Science*, vol. 325, no. 5945, pp. 1227–1230, Sep. 2009.
- [10] D. D. Awschalom, L. C. Bassett, A. S. Dzurak, E. L. Hu, and J. R. Petta, “Quantum spintronics: engineering and manipulating atom-like spins in semiconductors,” *Science*, vol. 339, no. 6124, pp. 1174–1179, Mar. 2013.
- [11] D. A. Steck, “Alkali D Line Data,” Oregon Center for Optics and Department of Physics, University of Oregon, 2001–[Online]. Available: <http://steck.us/alkalidata>.
- [12] G. J. Milburn, “Quantum optical tests of the Stern–Gerlach apparatus,” *J. Quantum Electron.*, vol. 36, no. 10, pp. 1061–1067, Oct. 2000.

### Information about authors:

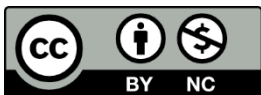
*Assel Akhmetova* – MS, Junior Researcher, Laboratory of Alternative Energy and Nanotechnology, Kazakh-British Technical University, Almaty, Kazakhstan, [assel.akhmetova.95@bk.ru](mailto:assel.akhmetova.95@bk.ru)

### Author Contributions:

*Assel Akhmetova* – concept, methodology, resources, data collection, testing, modeling, analysis, visualization, interpretation, drafting, editing, funding acquisition.

**Conflict of Interest:** The authors declare no conflict of interest.

**Use of Artificial Intelligence (AI):** The authors declare that AI was not used.



**Copyright:** © 2024 by the authors. Licensee Technobius, LLP, Astana, Republic of Kazakhstan. This article is an open access article distributed under the terms and conditions of the Creative Commons Attribution (CC BY-NC 4.0) license (<https://creativecommons.org/licenses/by-nc/4.0/>).